SAE International

Assessment of a Vehicle's Transient Aerodynamic Response

2012-01-0449
Published
04/16/2012

Nicholas Oettle, Oliver Mankowski, David Sims-Williams and Robert Dominy
Durham Univ

Claire Freeman and Adrian Gaylard
Jaguar Land Rover

doi:10.4271/2012-01-0449

ABSTRACT

A vehicle on the road encounters an unsteady flow due to turbulence in the natural wind, due to the unsteady wakes of other vehicles and as a result of traversing through the stationary wakes of roadside obstacles. There is increasing concern about potential differences between the steady flow conditions used for development and the transient conditions that occur on the road. This paper seeks to determine if measurements made under steady state conditions can be used to predict the aerodynamic behaviour of a vehicle on road in a gusty environment.

The project has included measurements in two full size wind tunnels, including using the Pininfarina TGS, steady-state and transient inlet simulations in Exa Powerflow, and a campaign of testing on-road and on-track. The particular focus of this paper is on steady wind tunnel measurements and on-road tests, representing the most established development environment and the environment experienced by the customer, respectively. Measurements of the surface pressure on the front sideglass were used for comparisons as this area exhibits a complex flow which is highly sensitive to yaw angle and which is also an important region, for wind noise considerations in particular.

It was found that, if the transient on-road environment is known then steady-state wind tunnel measurements can be used to predict accurately the transient surface pressures, provided the methodology is sufficiently rigorous. Admittance or transfer function techniques are commonly used to compare transient and steady-state results and the limitations of these methods are shown here when the spectra of self-excited and externally imposed unsteadiness overlap. A new method is introduced to obtain a "true" transfer or admittance function, unconfused by the presence of self-excited unsteadiness. The aerodynamic admittance was found to be close to unity up to a frequency of 2-10 Hz and it then drops progressively.

INTRODUCTION

A vehicle on the road encounters an unsteady flow due to turbulence in the natural wind, due to the unsteady wakes of other vehicles and as a result of traversing through the stationary wakes of roadside obstacles. There is no doubt that the time varying boundary conditions in this environment are very different to the steady state boundary conditions employed routinely in wind tunnels and computational fluid dynamics (CFD) simulation for vehicle aerodynamic development.

Vehicles experience a very wide range of conditions on-road. The assessment of the transient conditions experienced by a moving vehicle was pioneered by Watkins [1] and, for example Watkins, Saunders and Hoffmann [2]. The definitive work is that of Wordley [3] including [4], [5]. Other recent work includes that of Wojciak et al [6]. These and other studies are reviewed more completely by Howell [7], Cooper and Watkins [8] and Sims-Williams [9]. Two key points to note from these previous works on the on road environment are that:

1. Lateral velocity (yaw angle) fluctuations will be of greatest significance.

2. The greatest proportion of unsteadiness encountered will be below 10 Hz.

This paper seeks to determine if measurements made under steady state conditions can be used to predict the aerodynamic behaviour of a vehicle on road in a gusty environment. In this case transient surface pressures on the front sideglass are used as the basis for comparison. This provides an area of complex flow which is highly sensitive to yaw angle and which is important in particular from an aeroacoustic point of view.

If the vehicle response to an instantaneous condition (e.g. yaw angle) in a transient environment is the same as the response to the same condition in a steady environment then the response is termed quasi-steady. The reduced frequency is often used to characterise the rate of change in a transient in a non-dimensional way (discussed, for example, in [9, 10]. Reduced frequency is defined as:

$$K = \frac{\omega L}{U} = \frac{2\pi f L}{U} = \frac{2\pi L}{\lambda}$$

where ω is angular frequency (rad/s), f is frequency (Hz), L is a characteristic dimension of the geometry (vehicle length is used throughout this paper), U is free-stream velocity and λ is the turbulence wavelength (length scale).

EXPERIMENTAL METHOD

Measurements were made on the same vehicle in the Pininfarina wind tunnel and on the road, using a roof-mounted probe to record instantaneous conditions. Pressure taps were installed on a front sideglass and time-resolved pressures were recorded. Transient simulations were also performed in Exa Powerflow.

TEST VEHICLE

A vehicle typical of a European luxury saloon was used as the test vehicle, shown in Figure 1. As shown, a probe was mounted on the roof of the vehicle for the measurement of instantaneous flow conditions. The coordinate system that is used throughout the paper is shown in Figure 1 and Figure 2.

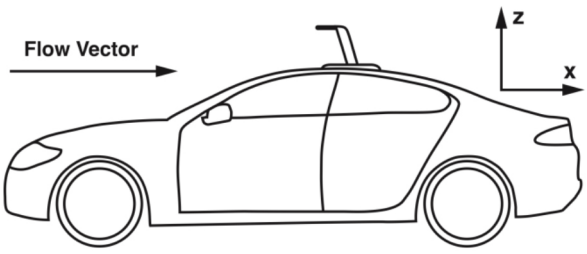

Figure 1. Test vehicle showing location of probe

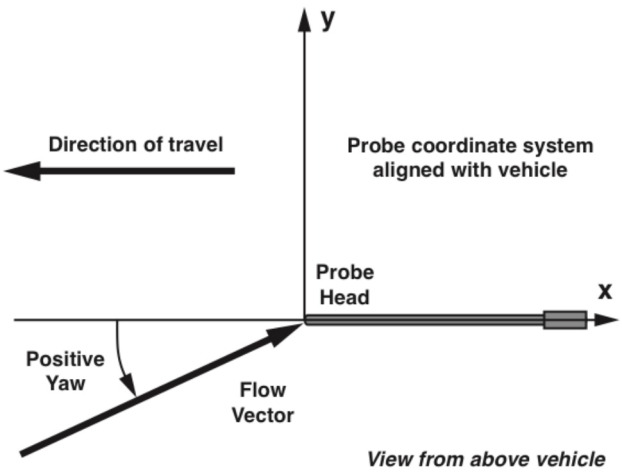

Figure 2. Plan view: Probe and vehicle coordinate system

ON-ROAD DATA COLLECTION

Roof Mounted Probe

To measure the flow over the vehicle, a roof-mounted 5-hole probe was used, as in Oettle et al [11, 12]. The probe tip was positioned approximately 320 mm above the vehicle's roofline, and approximately 70 mm in front of the B-pillar, as shown in Figure 1. The probe was manufactured and calibrated in isolation using facilities at Durham University. Five SensorTechnics HCLA12X5DB pressure transducers were used to measure the probe pressures. These measure differential pressure and have a range of ±12.5 mbar. The transducers were packaged into a single enclosure with a common reference and located within the probe mounting. The reference port was connected via a PVC tube to a location in the trunk of the vehicle. The probe mounting was attached to the roof of the vehicle magnetically.

A probe and tubing transfer function correction was applied, for magnitude and phase, to all on-road data for both the roof mounted five-hole probe and the sideglass pressure tappings. This is described by Irwin et al. [13] and implemented for probe measurements here by [14]. With the probe and remote transducers used in the investigation, this approach allows a frequency response in excess of 500 Hz. This significantly exceeds the required response for this application as higher frequency fluctuations contained in the wind are also correspondingly small in physical size and are therefore not correlated over the scale of the vehicle.

Any probe installation location will be a compromise between measuring the incoming flow that the vehicles sees, minimising the influence of the probe on the flow around the vehicle, and minimising the influence of the vehicle on the flow at the probe. Testing on public roads introduces additional constraints. A primary requirement for this work

was to avoid a measurable impact of the probe on the flow around the vehicle in the area being measured, in particular, for other aspects of the work, it was important that the probe had no impact on aeroacoustic measurements.

The approach used here (e.g. positioning the probe some distance off the vehicle and using a probe calibration performed in isolation rather than in situ) means that the yaw angles and other quantities reported are the actual values at the probe location and this is known with certainty. Steady state wind tunnel measurements show that the probe experiences a higher velocity flow than the driving velocity, and that the yaw angle at the probe is exaggerated at high yaw angles. While it may be tempting to "correct" for these effects in the results reported this would assume that the flow around the vehicle in a transient condition matches that in the steady state condition. This investigation concerns the comparison between the aerodynamic response of the vehicle under steady state and transient conditions and so such an assumption would not be appropriate a priori.

Sideglass Pressure Measurements

Pressures were measured on the front right (UK driver's side) sideglass. A Perspex sideglass was manufactured which matched the curvature of the original glass. Figure 3 - Location of selected window static pressure tappings Figure 3 illustrates the location of the tappings that are reported here. Each of these locations were drilled and 10 mm lengths of 1.24 mm OD stainless steel tubing was bonded in position, ensuring the outer surface of the sideglass remained smooth. The tubing inserts were each connected to separate SensorTechnics HCLA12X5DB pressure transducers located inside the cabin via PVC tubing. As for the probe measurement, pressures were measured relative to trunk pressure. Pressure coefficient cp was defined based on the static and dynamic pressure measured by the 5-hole probe. Again this provides something that is known with certainty in the on-road case as well as in the wind tunnel.

$$c_P = \frac{P_{\text{Tap}} - P_{\text{Probe Static}}}{\frac{1}{2}\rho U^2_{\text{Probe Resultant}}}$$

The relationship between the location of the pressure tappings and the yaw angle of the vehicle is shown in Figure 4, where "P" indicated the location of the instrumented sideglass.

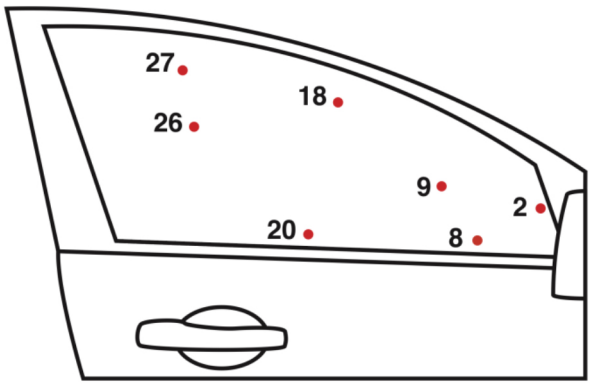

Figure 3. Location of selected window static pressure tappings

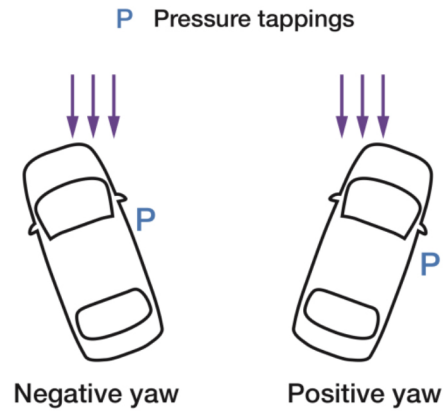

Figure 4. Definition of yaw angle showing location of pressure tappings

Data Acquisition

To log the output from the pressure transducers, a National Instruments NIDAQmx USB-6218 data logger was used. This was controlled by a laptop running control software developed in-house. Data were also received from a Bluetooth GPS device that was simultaneously logged with the pressure transducer data from the data logger using the same control software. The GPS data included details of the velocity and heading of the vehicle, in addition to information on the location of the vehicle and time of the experiment. The pressure transducer data were logged in sets of 16384 points at 500 Hz, therefore giving a logging duration of 32.768s. This logging time was considered suitable to capture the transient nature of the on-road environment. To avoid aliasing, the signal from each of the pressure transducers was passed through a 250 Hz second-order low-pass filter.

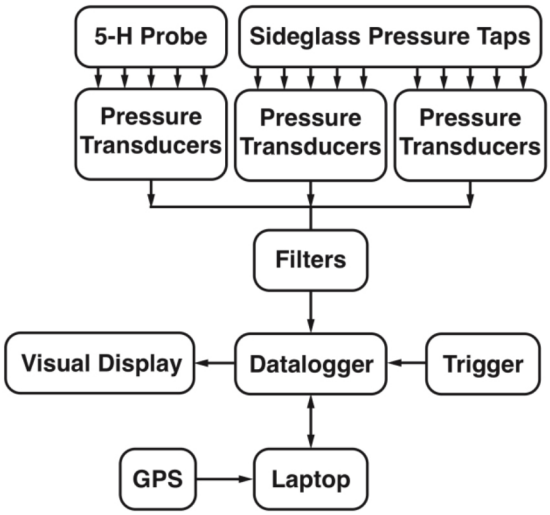

Figure 5. Schematic of logging system

The data logging system included a number of features to assist with the correlation between the data and the on-road environment, as well as the in-vehicle control of the system. An LED display was mounted on the dashboard of the vehicle, providing the driver with information on the logging status, GPS signal and run number. A video camera also recorded on-road events to further assist correlation between the external environment and the flow and noise data. An external trigger was used to start the logging system from within the vehicle. A schematic of the entire logging system is shown in Figure 5.

WIND TUNNEL

The same vehicle was tested in the Pininfarina wind tunnel. The same sideglass and probe were used to record data as on-road. The results reported here are all obtained with stationary ground and wheels and without the use of the Pininfarina turbulence generation system [15, 16]. Measurements were made at a range of turntable yaw angles from −20 degrees to +20 degrees at 2.5 degree increments. The wind tunnel velocity matched the on-road driving velocity. As discussed above, the yaw angles reported in the results correspond to those measured at the probe (as this is what is always known with certainty).

CFD SIMULATION

Simulations were performed using PowerFLOW 4.3b. This uses a special discretization of the Lattice-Boltzman method on a variable resolution Cartesian mesh (lattice). This approach is inherently time-dependent, whether the steady or time-varying inlet conditions are used. Further details are available in [17].

A base case was defined for all runs with no change in grid between simulations, with only the Y-velocity varying between any one simulation and another. Consideration was made to ensure that the finer mesh regions were sized to accommodate the maximum expected incoming flow yaw angle. Yawed flow was simulated by introducing yaw at the inlet and including periodic boundaries on either side of the domain, rather than by yawing the vehicle within the domain. Axial velocity was constant and the yaw angle variation was achieved by varying the lateral (and hence resultant) velocity. Obviously no symmetry plane was imposed.

Nine nested mesh refinement (Variable Resolution - VR) regions were established, each corresponding to a halving of cell linear dimension. Finer resolution meshes were used around the vehicle, including a 6mm vehicle wrap at a 20-lattice length offset and 3mm meshes around key vortex generating regions. In order to ensure that the balance between case accuracy and CPU time was optimised, a range of test cases were assessed prior to the final case design. The first objective was to minimise the harmonic inlet yaw attenuation downstream. While a large domain was used compared with the size of the vehicle, the domain width and distance between the inlet and model were smaller than other domain dimensions. Shortening this distance to the inlet reduced the required run time and minimised any distortion of the transient yaw profile. VR regions were staggered in coarseness in height and downstream to improve run times, but, importantly, were kept at the full domain width until at least after of the car model. As a result of the mesh refinement study, relatively fine cells (VR5, 48 mm/voxel) were used upstream of the vehicle extending from the inlet to a position downstream of the model. This is important to avoid any numerical blurring of the transient yaw profile. Cartesian projections of the VR region setup are visible in Figure 6 and Figure 7, below. Cases ran for 2.0s of physical time, with 380,000 time steps, averaging 1.31×10^{-5} s/timestep at VR9.

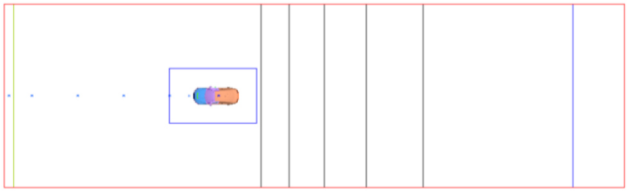

Figure 6. XY plane view of the Variable Resolution regions (VR0-6 being rectangular)

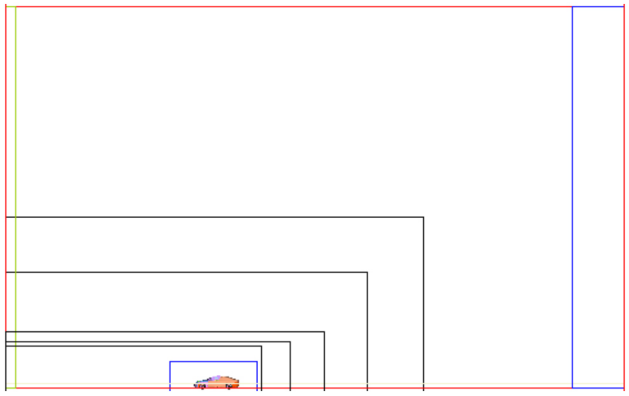

Figure 7. XZ Plane of the VR Regions. Note staggering of VR resolution in height and downstream of the model (VR0-6 being rectangular)

RESULTS

INVESTIGATION OF EFFECT OF PROBE LOCATION

CFD was used to investigate different probe locations, including locations that would not be practical on the road. A simulation was performed with a 2 Hz sinusoidal oscillation in lateral velocity at the inlet and the flow at different locations was noted. The yaw angle variation amplitude was 6 degrees. Figure 9 shows a comparison between the yaw angle observed at the location of the roof probe used here and in a location ahead of the vehicle, as used by Wordley [3] as shown in Figure 8. Both locations showed exaggerated lateral velocities; over the roof the axial velocity is also above the free stream value but ahead of the vehicle the axial velocity is below the free stream value. This means that ahead of the vehicle the observed yaw angle is exaggerated significantly.

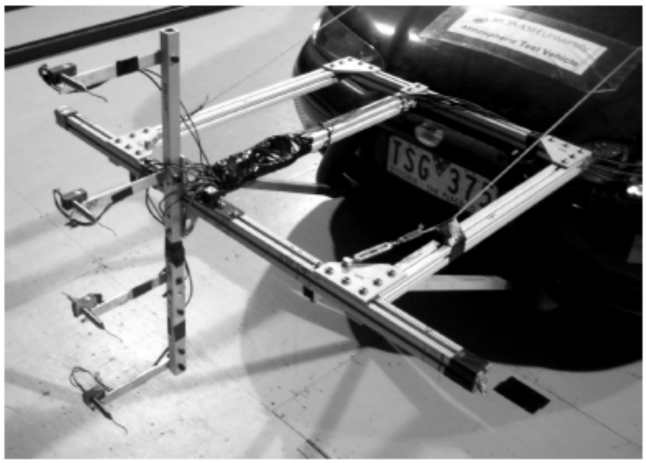

Figure 8. Probe mounted ahead of vehicle (Wordley [3])

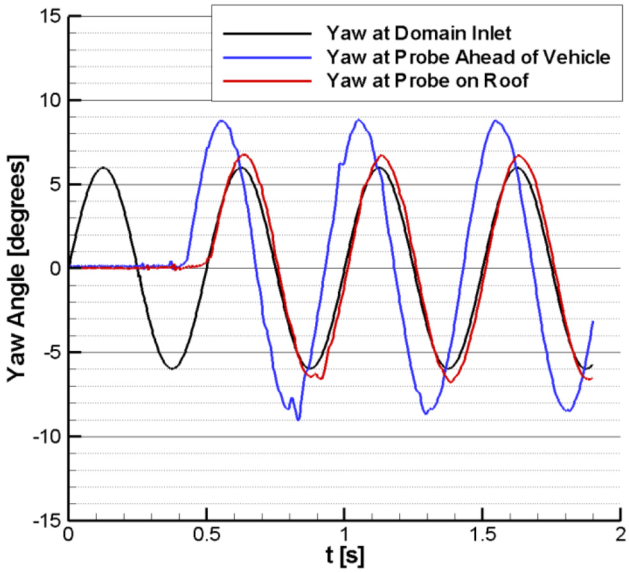

Figure 9. CFD: Yaw Angle vs Time at different locations

WIND TUNNEL MEASUREMENT OF SIDEGLASS PRESSURE VS YAW

Figure 10 and Figure 11 show sideglass cp values as recorded in the wind tunnel. The tapping locations have been sorted into these two figures based on their yaw response, which is in turn dependent on their location in the flow. The tappings presented in Figure 10 correspond to the mirror wake region and show generally decreasing cp with increasing yaw angle but with a plateau consistent with separated flow at larger positive yaw angles. Recall (referring to Figure 4) that positive yaw angle corresponds to these tappings being on the leeward side of the vehicle.

Figure 11 shows surface pressures in the area closer to the A-pillar and vortex reattachment region. These show a continuously decreasing pressure at increased yaw angles, including non-linearity consistent with the effect of longitudinal vortices (e.g. as per non-linear "vortex lift" generated by delta wings).

WIND TUNNEL PREDICTION OF TRANSIENT ON-ROAD SIDEGLASS PRESSURES

The wind tunnel provides the steady state vehicle aerodynamic response to yaw angle (in this case typified by the sideglass pressure coefficient vs. yaw angle). If the surface pressure coefficient experienced in transient (on-road) conditions for a particular instantaneous yaw angle matched that in the wind tunnel then the response can be described as quasi-steady.

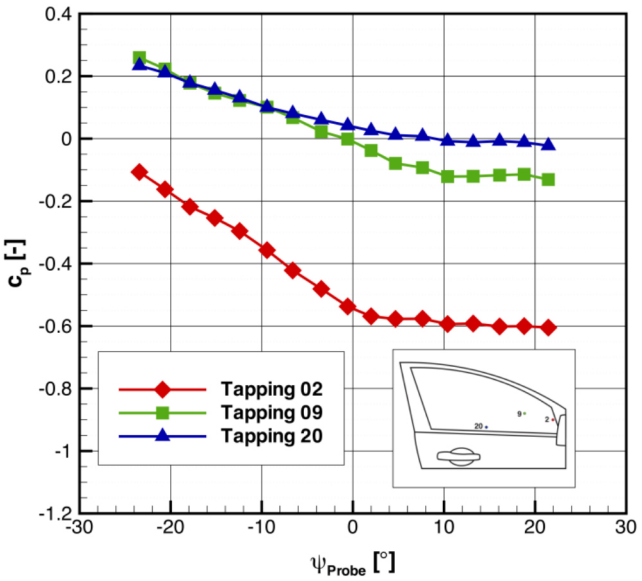

Figure 10. Wind tunnel sideglass pressures (mirror wake region)

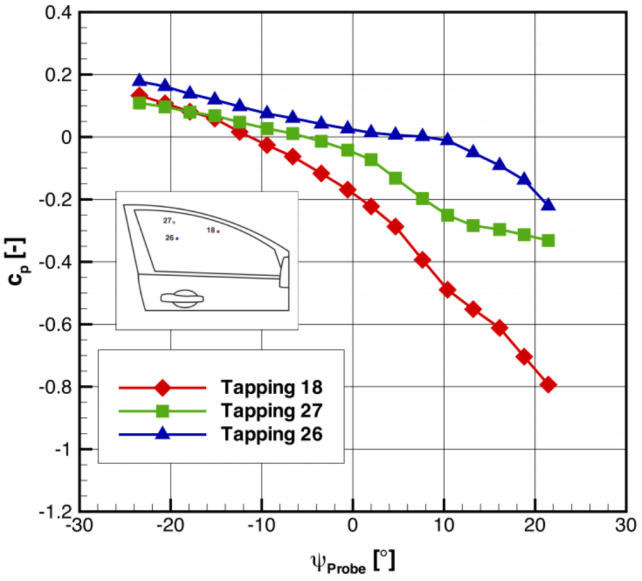

Figure 11. Wind tunnel sideglass pressures (vortex and reattachment region)

To assess the nature of the vehicle response, a simulation technique was implemented which used the c_p vs. yaw response measured in the wind tunnel combined with the measured transient flow characteristics measured by the probe on the vehicle roof on road to predict the instantaneous sideglass pressure. These predicted fluctuations in surface pressures were then assessed against those actually measured on-road. Figure 12 shows an example time trace for Tapping 9 and Figure 13 provides an illustration for Tapping 20.

It can be seen that the conventional wind tunnel measurements make it possible to successfully predict the transient surface pressure under on-road conditions, provided that the transient boundary conditions (yaw angle and resultant dynamic pressure vs. time as measured by the roof probe) are known. The agreements on transient aspects of the pressure are even better predicted than the steady state cp, as illustrated by the constant offset in Figure 13. It is worth highlighting that it is important to non-dimensionalise using the conditions at the roof probe in order to correctly account for changes in resultant velocity. A whole range of different resultant velocities are possible for the same driving velocity and resultant yaw angle (corresponding to different natural wind strengths and directions). Different resultant velocities will produce different absolute pressure levels and this must not be overlooked.

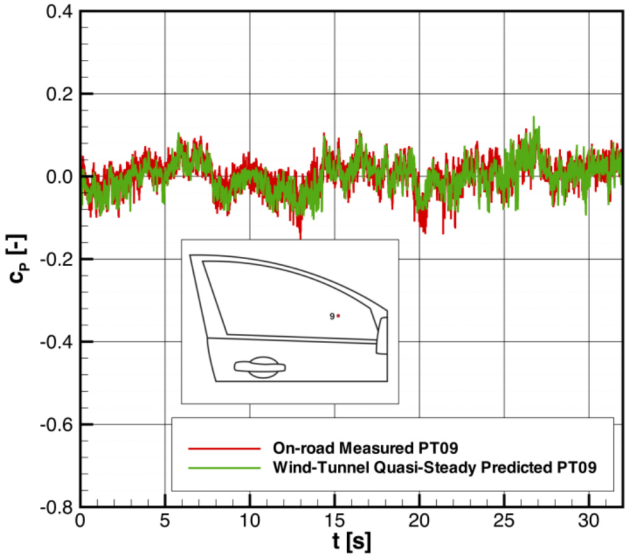

Figure 12. On-road surface pressures: Measured and predicted by wind tunnel (Tapping 9)

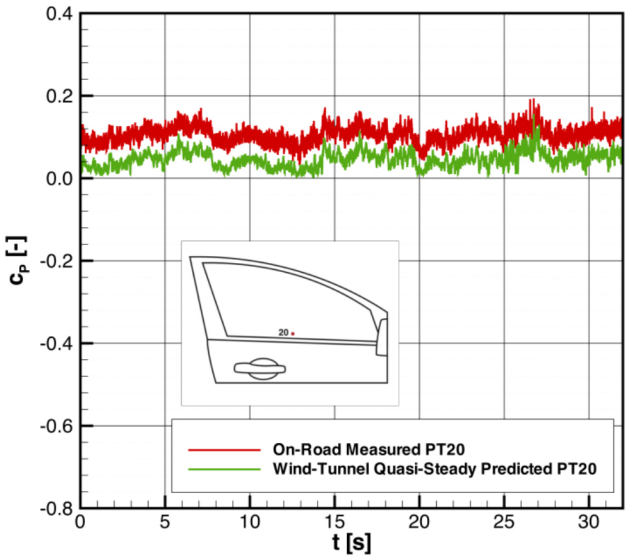

Figure 13. On-road surface pressures: Measured and predicted by the wind tunnel (Tapping 20)

Whilst the example time traces show a generally quasi-steady response, this was assessed formally through the use of transfer functions and spectral analysis to assess the quasi-steady response at the full range of unsteady fluctuation frequencies as measured on-road. The transfer function is defined according to Wordley [3] and is the ratio of the cross-spectral density of the measured and wind-tunnel-simulated pressures against the auto-spectral density of the simulated pressures. A transfer function of unity indicates that the sideglass fluctuations are as predicted in the wind tunnel. A shift in absolute cp values between those measured on-road and those measured in the wind tunnel, such as that shown by Tapping 20, would be manifested as a non-zero transfer function at low frequency (0 Hz), whilst not affecting the transfer function at higher frequencies.

$$H(f) = \frac{G_{SM}}{G_{SS}}$$

Transfer functions or aerodynamic admittance functions (fundamentally the same thing) are based on the expectation of a linear relationship between the two variables. Therefore the use of the wind-tunnel (quasi-steady) prediction in the transfer function has a couple of important advantages over other possible approaches (e.g. compared with defining a transfer function between yaw angle and surface cp). Using the wind tunnel predicted cp removes the non-linear dependence of surface pressure on yaw angle (e.g. as shown in Figure 10 and Figure 11). It also means that a quasi-steady response corresponds to a transfer function value of unity, as for aerodynamic admittance, without applying a "fix" to achieve this.

Figure 14 shows the spectral densities for pressure Tapping 9, based on many days of on-road measurements. As in Figure 12 and Figure 13 the two traces compare the actual surface pressure measured on road with that predicted by the cp vs. yaw curve measured in the wind tunnel, combined with the actual on-road variation in yaw and dynamic pressure measured by the probe on the roof. The progressive roll off of spectral energy as frequency increases can be clearly seen. The two spectra can be seen to agree very closely over most of the range but above 20 Hz, where the unsteadiness measured on the sideglass exceeds that predicted based solely on unsteadiness in the natural wind environment. The logical explanation is that there is energy contained within the

sideglass fluctuations that due to self-excited unsteadiness in the sideglass region (e.g. unsteady wake of the door mirror).

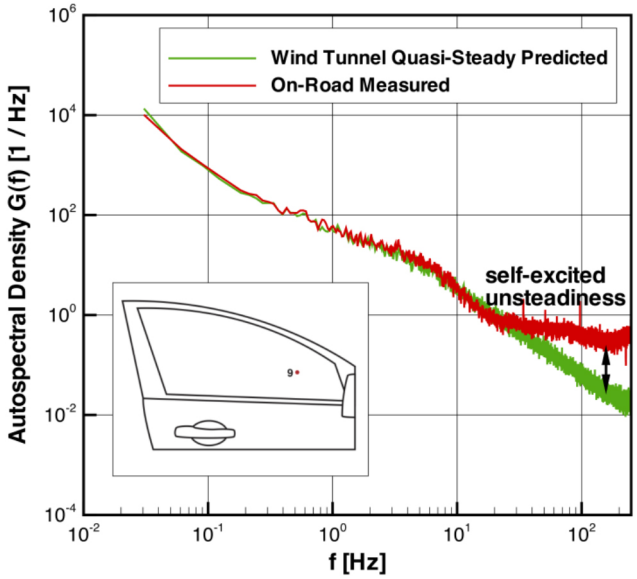

Figure 14. Spectral density for sideglass pressures on-road and predicted based on wind tunnel measurements (Tapping 9)

The transfer function is essentially a ratio (to the power one half) of the autospectral densities. Figure 15 and Figure 16 illustrate transfer functions for a selection of different sideglass pressure tappings and the behaviours in all cases are generally similar.

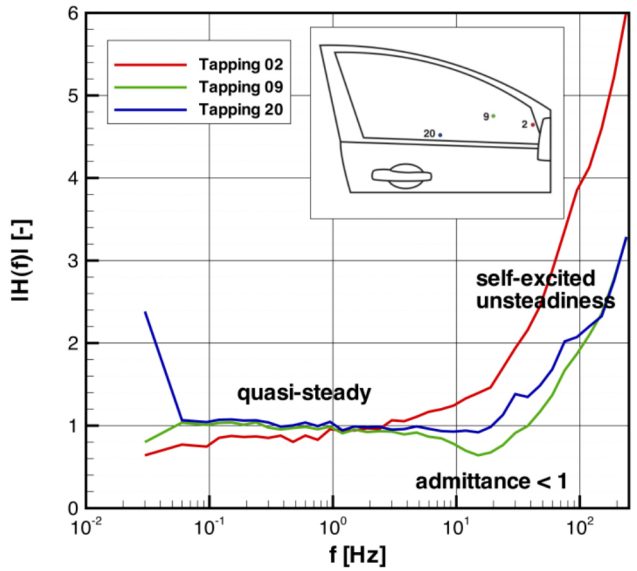

Figure 15. Wind tunnel to on-road transfer functions (mirror wake region)

At the lowest frequency, which is dictated by the length of the time record, there is generally a single non-unity point due to the steady-state difference in cp values between the on-road averaged measurements and those obtained in the wind tunnel. The value varies; depending on the sign of the cp values (and offset), this steady-state transfer function value can either be less than or greater than unity. If the wind-tunnel-predicted average cp value is close to zero then this can lead to a large steady-state value owing to this term being the denominator in the transfer function definition. Therefore this single steady-state value can exhibit a higher error and thus should be regarded with caution.

The most important observation is near unity transfer functions are seen at frequencies up to at least 2 Hz (K ~ 1), indicating a quasi-steady response over the frequency band where the majority of on-road unsteadiness is experienced. This shows that steady state wind tunnel tests, combined with knowledge of the environment to be experiences on-road, allows an accurate prediction of the surface pressures and hence transient forces etc. that can be expected.

In some cases, above 2-5 Hz, the transfer function decreases below unity, indicating that fluctuations measured by the probe are not translated to changes in surface pressure at the sideglass. This is consistent with the fact that the reduced frequency, K, is now greater than unity and so a quasi-steady response can no longer be expected.

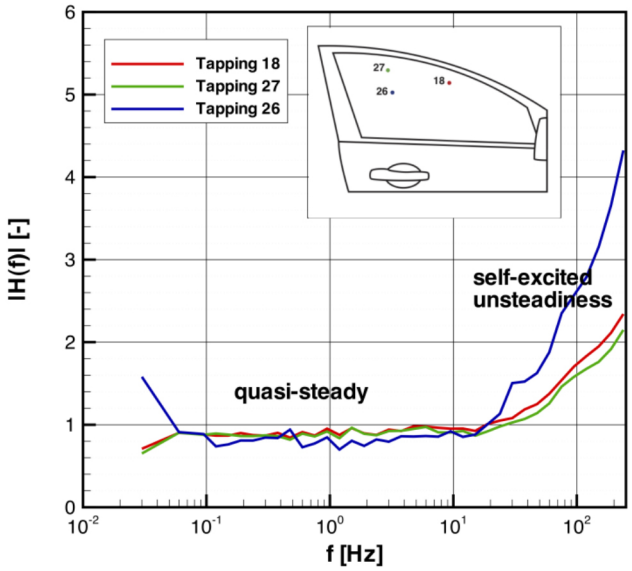

Figure 16. Wind tunnel to on-road transfer functions (vortex and reattachment region)

Beyond 10- 20 Hz the transfer functions increase rapidly above unity. While both the measured and wind-tunnel-simulated pressure fluctuations continue to decrease with frequency there is more fluctuation measured on the side glass on-road than predicted based on the yaw fluctuations seen at the probe and this is attributed to self-excited unsteadiness. Tapping 2 is closely positioned to the door

mirror and stem assembly and is therefore correspondingly more affected by the self-excited flow structures being shed from the mirror. This is shown by the rapid increase in transfer function at 2 Hz. Tappings 18 and 27, as shown by Figure 16, appear to show the least self-excited effects owing to their location furthest away from the mirror wake.

CFD SIMULATION OF 2 HZ YAW VARIATION

Noting that the upper limit for quasi-steady behaviour could be in the region of 2 Hz, a CFD simulation was performed with varying inlet yaw angle at a frequency of 2 Hz. The instantaneous conditions at the location of the roof probe were used to calculate the expected surface pressure coefficient based on the wind tunnel measurements and the assumption of quasi-steady behaviour. The comparison between this wind tunnel prediction and the CFD result for a tapping in the A-pillar vortex region is shown in Figure 17. In this location the CFD predicted an average pressure lower than the wind tunnel and an unsteady amplitude below the quasi-steady prediction. This corresponds to a transfer function at 2 Hz of about 0.6 but the result for different tappings varied significantly.

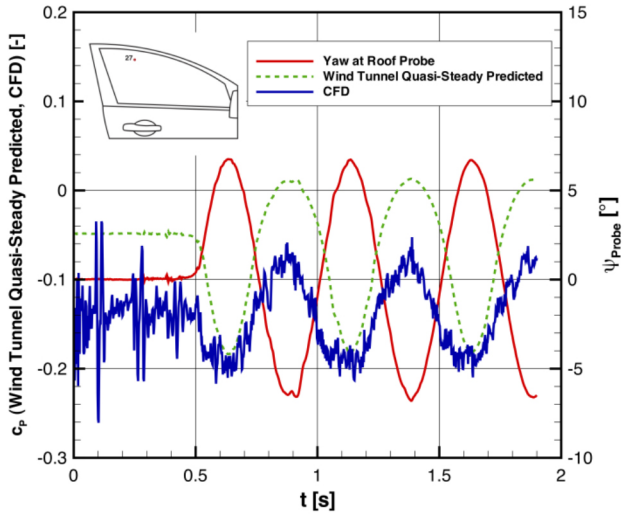

Figure 17. CFD Simulation of Yaw Variation at 2 Hz: Cp from CFD compared with the Wind Tunnel Quasi-Steady Prediction

For the same case and tapping, Figure 18 plots the pressure coefficient simulated by CFD directly against that predicted by the wind tunnel; two complete cycles are plotted. In general this figure shows a slope generally less than unity, corresponding to a transfer function less than unity. The slope varies through the cycle and is close to unity at the highest pressures (when the tapping is on the windward side of the vehicle) and the slope is lowest on when the tapping is on the leeward side of the vehicle. This suggests that the flow deviates most from quasi-steady behaviour in the leeward region but this result is not sufficiently validated to be confident in that supposition. This figure also shows some difference in pressure at the same instantaneous yaw angle, depending on whether the yaw angle is increasing or decreasing but again care needs to be taken as the results for different tapping locations was not consistent.

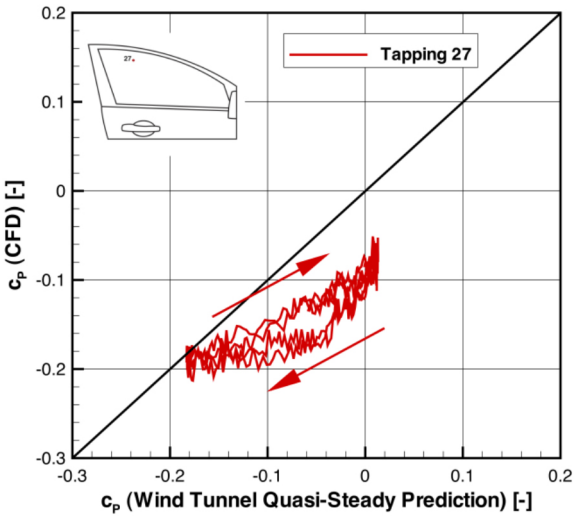

Figure 18. CFD Simulation of Yaw Variation at 2 Hz: Cp from CFD vs. Wind Tunnel Quasi-Steady Prediction

SEPARATING EXTERNALLY-IMPOSED AND SELF-EXCITED UNSTEADINESS

In order to better elucidate the impacts of externally-imposed unsteadiness and self-excited unsteadiness the on-road measured and wind-tunnel-predicted records of surface pressure were put through spectral filters and then the remaining level of unsteadiness (cp standard deviation) was computed. Figure 19 presents the level of unsteadiness between 0.1 Hz and 10 Hz and plots the level measured on road compared with that predicted by the wind tunnel. Each point corresponds to a different on-road record. It can be seen that overall, the agreement is excellent.

Figure 20 presents the corresponding data for a frequency band from 10 Hz to 250 Hz, where self-excited unsteadiness takes on increasing importance compared with externally-imposed unsteadiness. What is seen here is that the actual level of sideglass unsteadiness has a baseline level (dictated by self-excited unsteadiness) as well as a small dependence on external effects.

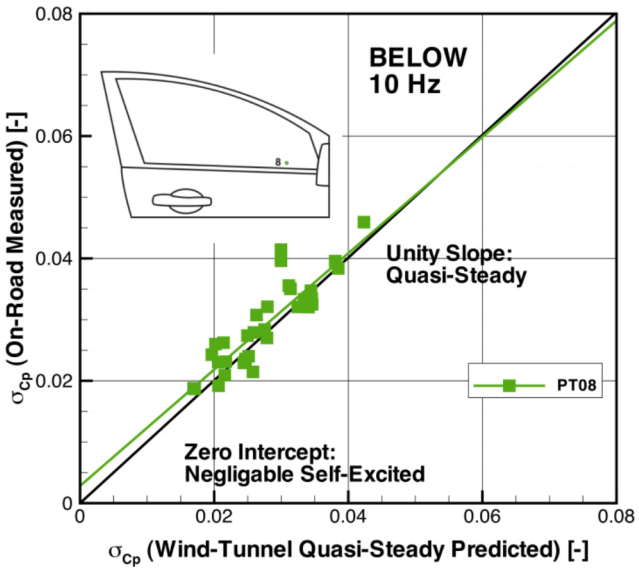

Figure 19. 0.1Hz-10Hz: Cp Fluctuation Measured On-Road vs. Wind Tunnel Quasi-Steady Prediction

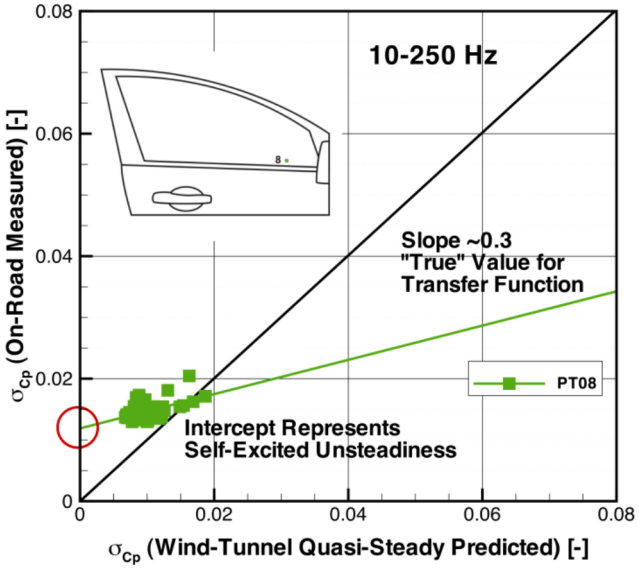

Figure 20. 10Hz-250Hz: Cp Fluctuation Measured On-Road vs. Wind Tunnel Quasi-Steady Prediction

If we represent the unsteady aerodynamic response conventionally, using an admittance or transfer function, then we are effectively computing the slope for a family of plots like Figure 19 and Figure 20 but in each case forcing an intercept of (0,0) and taking the slope to the centre of the cluster of points. This is fine for cases where almost all of the unsteadiness is caused by the external source (as in Figure 19) but produces misleading results where there is a combination of sources of unsteadiness. A better representation is achieved by separately looking at the intercept and slope of a line through the points, as drawn on these two figures. The y-axis intercept of these lines represents the level of self-excited unsteadiness while the slope of this line represents the response of the vehicle to the externally-imposed unsteadiness. Looking at Figure 20 we see self-excited unsteadiness a little greater than 1% of resultant dynamic pressure with a slope of 0.3, indicating that at these higher frequencies about 30% of the unsteadiness predicted by a quasi-steady approach due to externally-imposed fluctuations actually gets translated through to sideglass pressure fluctuations.

This technique can be extended by determining the slope and intercept of a number of frequency bands to build up a "true" transfer function, unconfused by the presence of self-excited unsteadiness. Figure 21 shows the comparison between the data obtained using the new method with that of a conventional transfer function. Four frequency bands were chosen, equally logarithmically spaced between 0.1 Hz and 250 Hz.

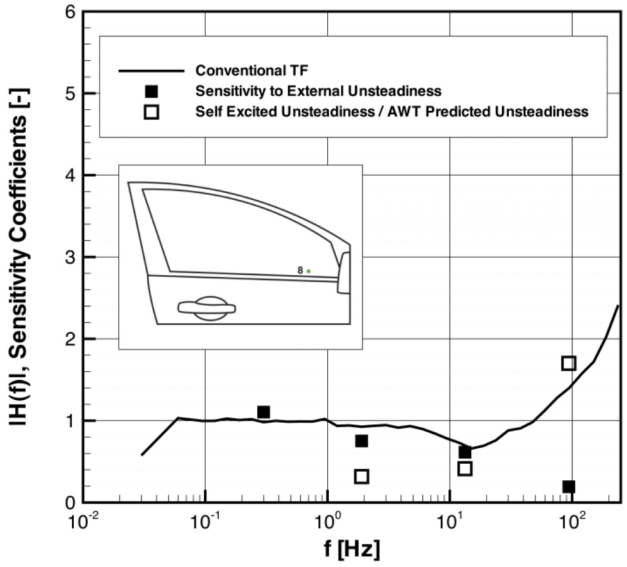

Figure 21. Separated Externally Imposed Unsteadiness and Self-Excited Unsteadiness Response Functions

The sensitivity to external unsteadiness, as determined using the same slope method as shown in Figure 19 and Figure 20, but with these more closely spaced frequency bands is plotted against the conventional transfer function. Up until approximately 10 Hz, the result from this method and a conventional transfer function agree closely. Above this frequency the new method reveals that progressively less of the energy contained within the external unsteadiness is transmitted to unsteadiness measured on the sideglass. The method also allows extraction of the self-excited contribution to the unsteadiness. The self-excited contribution for each frequency band is also shown in Figure 21, described by the intercept as a proportion of the unsteadiness predicted by the wind tunnel method. At the lowest frequency band, the self-excited contribution is negligible and this increases

progressively showing that self-excited effects begin to dominate over externally imposed unsteadiness above about 10 Hz.

CONCLUSIONS

A quasi-steady technique combining steady state wind tunnel measurements with measurements of the fluctuating yaw angle and resultant velocity experienced by a vehicle on road has been demonstrated to predict sideglass pressure transients with high fidelity.

At highway speed, the vehicle aerodynamic response (characterised by front sideglass pressure) remained quasi-steady up to at least 2 Hz (K = 1).

At frequencies above 10-20 Hz there is very little unsteady energy in the on-road environment and self-excited unsteadiness (e.g. due to the wing mirror) dominates the unsteadiness on the sideglass.

A new method is introduced for separating the effects of externally imposed unsteadiness and self-excited unsteadiness in order to obtain a "true" transfer or admittance function, unconfused by the presence of self-excited unsteadiness. This method indicates that the aerodynamic admittance drops below unity above a frequency of 2-10 Hz and has dropped to less than 0.2 by 100 Hz.

REFERENCES

1. Watkins, S, Wind-Tunnel Modelling of Vehicle Aerodynamics: With Emphasis on Turbulent Wind Effects on Commercial Vehicle Drag, PhD Thesis, Victorian University of Technology, 1990.

2. Watkins, S, Saunders, J, Hoffmann, P, Turbulence Experienced by Moving Vehicles. Part 1. Introduction and Turbulence Intensity, Journal of Wind Engineering and Industrial Aerodynamics, 1995. **57**(1-17)

3. Wordley, S, On-Road Turbulence, PhD Thesis, Monash University, 2009.

4. Wordley, S. and Saunders, J., "On-road Turbulence," *SAE Int. J. Passeng. Cars - Mech. Syst.* 1(1):341-360, 2009, doi: 10.4271/2008-01-0475.

5. Wordley, S. and Saunders, J., "On-road Turbulence: Part 2," *SAE Int. J. Passeng. Cars - Mech. Syst.* 2(1):111-137, 2009, doi:10.4271/2009-01-0002.

6. Wojciak, J, Indinger, T, Adams, N, Theissen, P, Demuth, R. Experimental Study of on-Road Aerodynamics During Crosswind Gusts, MIRA Vehicle Aerodynamics Conference. Grove, UK, 2010.

7. Howell, J. Real Environment for Vehicles on the Road, Euromotor - Progress in Vehicle Aerodynamics. Stuttgart, 2000.

8. Cooper, K. and Watkins, S., "The Unsteady Wind Environment of Road Vehicles, Part One: A Review of the On-road Turbulent Wind Environment," SAE Technical Paper 2007-01-1236, 2007, doi:10.4271/2007-01-1236.

9. Sims-Williams, D., "Cross Winds and Transients: Reality, Simulation and Effects," *SAE Int. J. of Passeng. Cars - Mech. Syst.* 4(1):172-183, 2011, doi:10.4271/2011-01-0172.

10. He, L, Modelling Issues for Computation of Unsteady Turbomachinery Flows, Lecture Series 1996-05, Unsteady Flows in Turbomachines. Von Karman Institute for Fluid Dynamics 1996

11. Oettle, N., Sims-Williams, D., Dominy, R., Darlington, C. et al., "The Effects of Unsteady On-Road Flow Conditions on Cabin Noise," SAE Technical Paper 2010-01-0289, 2010, doi:10.4271/2010-01-0289.

12. Oettle, N., Sims-Williams, D., Dominy, R., Darlington, C. et al., "The Effects of Unsteady On-Road Flow Conditions on Cabin Noise: Spectral and Geometric Dependence," *SAE Int. J. of Passeng. Cars - Mech. Syst.* 4(1):120-130, 2011, doi:10.4271/2011-01-0159.

13. Irwin, H, Cooper, K, Girard, R, Correction of Distortion Effects Caused by Tubing Systems in Measurements of Fluctuating Pressures, Journal of Industrial Aerodynamics, 1979. **5**(1-2), p. 93-107

14. Sims-Williams, D. and Dominy, R., "Experimental Investigation into Unsteadiness and Instability in Passenger Car Aerodynamics," SAE Technical Paper 980391, 1998, doi: 10.4271/980391.

15. Cogotti, A., "Generation of a Controlled Level of Turbulence in the Pininfarina Wind Tunnel for the Measurement of Unsteady Aerodynamics and Aeroacoustics," SAE Technical Paper 2003-01-0430, 2003, doi:10.4271/2003-01-0430.

16. Cogotti, A., "Update on the Pininfarina "Turbulence Generation System" and its Effects on the Car Aerodynamics and Aeroacoustics," SAE Technical Paper 2004-01-0807, 2004, doi:10.4271/2004-01-0807.

17. Lietz, R., Mallick, S., Kandasamy, S., and Chen, H., "Exterior Airflow Simulations Using a Lattice Boltzmann Approach," SAE Technical Paper 2002-01-0596, 2002, doi: 10.4271/2002-01-0596.

CONTACT INFORMATION

Dr David Sims-Williams
School of Engineering & Computer Sciences
Durham University
South Road, Durham, UK DH1 3LE

ACKNOWLEDGMENTS

The authors are grateful to Jaguar Land Rover for supporting this work, and for permission to publish, to EPSRC and

SCAST for supporting the lead authors, to Joaquin Gargoloff at Exa Corporation for his advice and assistance and to the staff at Pininfarina for supporting the wind tunnel test portion of this work.

DEFINITIONS/ABBREVIATIONS

c_P
Pressure Coefficient

f
Frequency (Hz)

G(f)
Spectrum (autospectral density) at f

H(f)
Transfer function at frequency f

K
Reduced frequency

L
Vehicle Length (characteristic dimension)

p
Pressure (Pa)

t
Time (s)

u
Velocity (m/s)

x
Axial direction (aligned with vehicle).

y
Lateral direction.

λ
Turbulence wavelength (length scale)

ω
Angular Frequency (rad/s)

CFD
Computational Fluid Dynamics

TGS
Turbulence Generation System

The Engineering Meetings Board has approved this paper for publication. It has successfully completed SAE's peer review process under the supervision of the session organizer. This process requires a minimum of three (3) reviews by industry experts.

ISSN 0148-7191

SAE Customer Service:
Tel: 877-606-7323 (inside USA and Canada)
Tel: 724-776-4970 (outside USA)
Fax: 724-776-0790
Email: CustomerService@sae.org
SAE Web Address: http://www.sae.org
Printed in USA